

# Modeling Bipolar Phase-Shifted Multielectrode Catheter Ablation

Supan Tungjitkusolmun, *Member, IEEE*, Dieter Haemmerich, *Student Member, IEEE*,  
Hong Cao, *Student Member, IEEE*, Jang-Zern Tsai, *Student Member, IEEE*, Young Bin Choy, *Student Member, IEEE*,  
Vicken R. Vorperian, and John G. Webster\*, *Life Fellow, IEEE*

**Abstract**—Atrial fibrillation (AFIB) is a common clinical problem affecting approximately 0.5–1% of the United States population. Radio-frequency (RF) multielectrode catheter (MEC) ablation has successes in curing AFIB. We utilized finite-element method analysis to determine the myocardial temperature distribution after 30 s, 80 °C temperature-controlled unipolar ablation using three 7F 12.5-mm electrodes with 2-mm interelectrode spacing MEC. Numerical results demonstrated that cold spots occurred at the edges of the middle electrode and hot spots at the side electrodes. We introduced the bipolar phase-shifted technique for RF energy delivery of MEC ablation. We determined the optimal phase-shift ( $\phi$ ) between the two sinusoidal voltage sources of a simplified two-dimensional finite-element model. At the optimal  $\phi$ , we can achieve a temperature distribution that minimizes the difference between temperatures at electrode edges. We also studied the effects of myocardial electric conductivity ( $\sigma$ ), thermal conductivity ( $k$ ), and the electrode spacing on the optimal  $\phi$ . When we varied  $\sigma$  and  $k$  from 50% to 150%, optimal  $\phi$  ranged from 29.5° to 23.5°, and in the vicinity of 26.5°, respectively. The optimal  $\phi$  for 3-mm spacing MEC was 30.5°. We show the design of a simplified bipolar phase-shifted MEC ablation system.

**Index Terms**—Bipolar ablation, cardiac ablation, catheter ablation, finite-element, phase-shift, radiofrequency ablation.

## I. INTRODUCTION

**A**TRIAL fibrillation (AFIB) is the most common sustained cardiac arrhythmia—it affects approximately 0.5%–1% of the U.S. population, and over 10% of those over 60 years old [1], [2]. The number of patients suffering from this arrhythmia will continue to increase as the general population ages in the future. Common symptoms for those affected by AFIB include unpleasant irregular heartbeats, impaired hemodynamics caused by loss of atrioventricular (AV) synchrony and vulnerability to thromboembolic complications [3]. One of the conventional therapies for AFIB is using antiarrhythmic drugs. However, this

approach is associated with high recurrence and adverse effects [22]. To achieve heart rate control in AFIB, AV nodal ablation with pacemaker insertion can help create heart block with regulation of the cardiac rhythm via ventricular pacing. However, the risk of thromboembolism remains unchanged because the atria continue to fibrillate.

The standard 4-mm electrodes utilized for radio-frequency (RF) ablation are capable of forming discreet spheroid shaped lesions of limited maximal diameter (10–12 mm). These lesions are adequate for the elimination of discreet focal arrhythmia substrates, however, they are inadequate when cardiac tissue of larger volume or of elongated geometry needs to be ablated. It has been demonstrated that the creation of long and continuous linear lesions in the right and left atrium and around the ostium of the pulmonary veins may cure AFIB [4], [5]. Similarly, in a more organized form of very rapid atrial arrhythmia called atrial flutter, which may sometimes be a precursor of AFIB, it has been demonstrated that a single linear lesion in the right atrium may cure atrial flutter. However, creation of such linear lesions with standard 4-mm tip catheters is fraught with difficulty. For example, during to cure typical atrial flutter, a line of block is created in the inferior vena cava-tricuspid annulus isthmus by dragging a conventional ablation catheter, stabilized by an elongated sheath, along the desired line. Atrial flutter may recur in up to 20% of patients because of recovery of conduction across the isthmus and incomplete linear lesion formation presence of “gaps” and inadequate ablation. Moreover, the procedure is time-consuming, and technically difficult because of the inadequacy of the tools utilized.

Subsequently, catheters with multiple electrodes with specific electrode spacing were developed. Throughout the past few years, the feasibility of the multielectrode catheter (MEC) approach to create linear lesions has been demonstrated in a number of animal and human studies [6]–[8]. New mapping technologies have also been developed to assist electrode placement in the cardiac chambers [9].

Some new power delivery schemes for RF ablation have also been introduced in recent years. Goldberg *et al.* developed a computerized algorithm for pulsed, high-current percutaneous RF hepatic ablation, which maximally increases the extent of induced coagulation necrosis [10]. Sun studied a multielectrode finite-element method (FEM) model and compared the lesion dimensions during phased linear AFIB ablation and found that ablation with a 90° angle improved lesion depth and continuity in constant power ablation during the initial 60 s [11]. When ablation time was longer than 120 s, the lesion depth and continuity

Manuscript received September 9, 2000; revised August 15, 2001. This work was supported by the National Institutes of Health (NIH) under Grant HL56143. Asterisk indicates corresponding author.

S. Tungjitkusolmun is with the Department of Electronics Engineering, King Mongkut's Institute of Technology Ladkrabang, Chalokkrung Rd., Ladkrabang, Bangkok 10520, Thailand.

D. Haemmerich is with the Department of Biomedical Engineering, University of Wisconsin, Madison, WI 53706 USA.

H. Cao, J.-Z. Tsai and Y. B. Choy are with the Department of Electrical and Computer Engineering, University of Wisconsin, Madison, WI 53706 USA.

V. R. Vorperian is with the Department of Medicine, University of Wisconsin, Madison, WI 53792 USA.

\*J. G. Webster Department of Biomedical Engineering, University of Wisconsin, 1415 Engineering Dr., Madison, WI 53706 USA (email: webster@engr.wisc.edu).

Publisher Item Identifier S 0018-9294(02)00202-1.

TABLE I  
THERMAL AND ELECTRICAL PROPERTIES OF THE MATERIALS IN THE FINITE-ELEMENT MODELS

FEM region	Material	$\rho$ (g·mm <sup>-3</sup> )	$c$ (J·g <sup>-1</sup> ·K <sup>-1</sup> )	$k$ (W·mm <sup>-1</sup> ·K <sup>-1</sup> )	$\sigma$ (S mm <sup>-1</sup> )
Blood	Blood	10 <sup>-3</sup>	4.18	5.43×10 <sup>-4</sup>	6.67×10 <sup>-4</sup>
Catheter body	Polyurethane	7×10 <sup>-5</sup>	1.045	2.6×10 <sup>-5</sup>	10 <sup>-8</sup>
Coating	UV adhesive	3.2×10 <sup>-5</sup>	8.35×10 <sup>-1</sup>	3.8×10 <sup>-5</sup>	10 <sup>-8</sup>
Electrode	Stainless steel	8×10 <sup>-3</sup>	4.8×10 <sup>-1</sup>	1.5×10 <sup>-2</sup>	7.4×10 <sup>-3</sup>
Tissue	Cardiac muscle	1.2×10 <sup>-3</sup>	3.2	5.5×10 <sup>-4</sup>	2.22×10 <sup>-4</sup>

were slightly different from the values observed when using 0° angle. Panescu *et al.* presented *in vitro* and *in vivo* studies of current densities and thermal profiles generated by MEC [12] for long multielectrode structures, and the mechanical features of a steerable catheter and performance of a multielectrode multitemperature-sensor temperature controller. Zheng *et al.* performed *in vivo* ablation on pig thigh muscle with a six-electrode linear catheter. They found phased application with 127° angle and 130° angle between the voltage of adjacent electrodes created deeper and more uniform lesions than monopolar (between electrodes and groundpad) [18], [19]. Hall *et al.* created linear lesions *in vivo* in canines using phased MEC [20]. Walcott *et al.* successfully created linear lesions in ten patients using a 12-electrode phased MEC [21].

RF energy is a form of electromagnetic energy that has been used for a variety of medical applications. The energy used in catheter ablation applications generally utilizes frequencies of 300 kHz to 1 MHz. RF current is routinely delivered via the electrode of an ablation catheter and a ground electrode applied to the subject's dorsal side. Myocardial injury occurs once a temperature of approximately 50 °C has been reached [13]. However, the tissue temperature should be kept below 100 °C to prevent charring, desiccation, and popping [23]. Popping occurs, when temperatures above 100 °C are reached, and water starts to boil and vaporize.

Current ablation catheters are affected by the edge effect—the formation of hot spots along the junction of the metal electrode with the insulating catheter—due to a sudden shift of electrical properties at the boundary [12], [14].

In this paper, we use FEM analysis to determine the temperature distribution in myocardium created by three-segment MEC RF ablation. We begin with a three-dimensional (3-D) FEM model of unipolar MEC ablation. Next, we introduce a RF energy delivery scheme for bipolar phase-shifted MEC ablation. For this technique, we use two sinusoidal constant voltage sources. One of the voltage sources is applied to the middle electrode (B), while the other is phase-shifted and applied to the side electrodes (A and C). Due to computation time limit, we utilize a two-dimensional (2-D) model to determine the optimal phase-shift where the temperatures at the edges of the three electrodes are equal. Reported myocardial properties in the literature vary significantly. This might be both due to measurement error, and due to interpatient and inpatient variability. To study the impact of change in myocardial properties on optimal phase-shift we also study the effects of the myocardial electric conductivity, and thermal conductivity, and the inter-electrode spacing on the optimal phase. Furthermore, we study

the effect of change in interelectrode spacing. We present a simplified block diagram for a bipolar phase-shifted MEC ablation system in Section IV.

## II. METHODS

### A. FEM Modeling of RF Ablation Using MEC

Mathematical modeling is a powerful tool for predicting lesion dimensions created by various electrode designs. In order to determine the change in temperature distributions in myocardium during ablation, we solved the bio-heat equation, which was first introduced by Pennes [24]. The FEM representation facilitates the computation of the temperature distribution over the entire mesh at each time step by reducing the bio-heat equation to a system of simultaneous equations that can be represented as a standard matrix equation. We have utilized the FEM analysis to study several electrode designs such as needle electrodes, and uniform current density electrodes [14], [15].

Panescu *et al.* described the structures and the controlling mechanism of a typical MEC ablation system that had bidirectional steering and carried up to six 7F 12.5-mm-long metal coil electrodes [12]. The system was capable of delivering RF power simultaneously to any user-selected combination of coils. Temperatures measured by thermal sensors at all of the selected coil electrodes were processed by a microcontroller, which provided the maximum value to the generator. The generator adjusted the delivered power to maintain the temperature at the preset level. We constructed our 2-D and 3-D FEM models based on the system structures described above by Panescu *et al.*

We used MSC/PATRAN v.7.0 (The MacNeal-Schwendler Co., Los Angeles, CA) for mesh generation and ABAQUS v.5.8 (Hibbitt, Karlsson & Sorensen, Inc., Farmington Hills, MI) for solution and postprocessing on a HP C180 UNIX workstation with 1,152-MB RAM and 34-GB hard disk. Table I lists the material properties used in this study [12].

All models were designed to have nonuniform meshes that provided better numerical accuracy at regions near the electrode edges where we expected more rapid variations of current density and temperature. The goals of the FEM analyses in this study were to determine the following: 1) The temperature distribution in myocardium produced by unipolar MEC ablation using a 3-D FEM model. 2) The optimal phase-shift between the two voltage sources that created uniform temperatures at all electrode edges in bipolar MEC using a 2-D FEM model. 3) The effects of changes in myocardial properties (electric conductivity, and thermal conductivity) to the optimal phase using

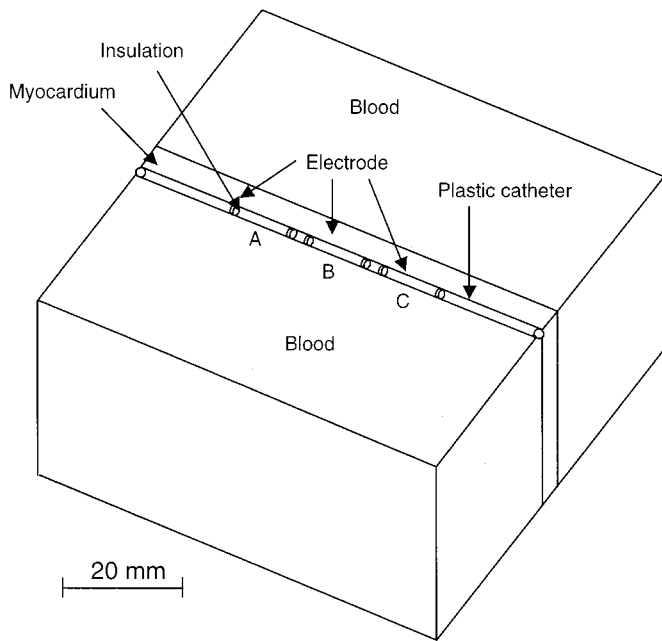


Fig. 1. The 3-D model includes three 7F-12.5-mm-long electrodes, myocardium, blood and the plastic catheter. Electrode B is in the middle, while electrodes A and C are on the side.

a 2-D FEM model. 4). The optimal phase for the MEC with 3-mm electrode spacing using a 2-D FEM model.

### B. Myocardial Temperature Distribution in 3-D Unipolar MEC System

The purpose of this simulation was to demonstrate that the edge effect also occurs at the edges of the metal electrodes in unipolar MEC ablation. In order to determine the temperature distribution in myocardium during MEC ablation, we constructed a 3-D FEM model that included myocardium, catheter body with a diameter size of 2.3 mm (7F), three 7F 12.5-mm electrodes with 2-mm interelectrode spacing, and blood. Fig. 1 shows the bottom half of the overall parallelepiped geometry of our 3-D model. The catheter was halfway embedded (penetration depth = 1.15 mm) into the 8-mm-thick myocardium, and the blood pool surrounds the myocardium. We also included the insulation at the edges of the electrodes. This 3-D model had 273 412 tetrahedral elements and 62 102 nodes.

We assigned appropriate boundary and initial conditions to the FEM model [14], [15]. Ground potential was assigned to all outer surfaces of the blood volumes. In unipolar temperature-controlled RF ablation, we adjusted the amplitude of the voltage source on the surfaces of the cylindrical electrodes (A, B, and C) until we obtained the preset maximum temperature value (but always applied the same voltages to the three electrodes). For this study, the ablation duration was 30 s, and the preset temperature was 80 °C. The time step size was between 0.1 and 2 s. We adjusted the voltage amplitude after each time step by trial and error to maintain 80 °C maximum myocardial temperature for the entire duration. This technique has been used previously [24].

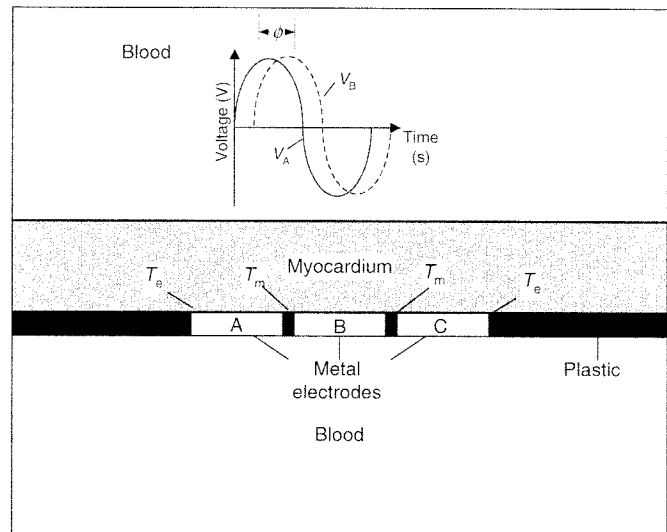


Fig. 2. The simplified 2-D FEM model also includes three metal electrodes in the model (A and C on the left and right sides, and B in the middle). The sinusoidal voltages were applied to the electrodes ( $V_A$  for A and C, and  $V_B$  for B).  $T_e$  is the temperature at the outer edges of A and C, and  $T_m$  is the temperature at the edges of electrode B. The phase-shift between the two voltage sources is  $\phi$ .

### C. Determining an Optimal Phase-Shift in a Simplified 2-D Bipolar Phase-Shifted MEC

For bipolar phase-shift RF ablation, we needed to apply different ac voltages to the electrodes. The purpose of this analysis was to demonstrate that the optimal phase-shift ( $\phi$ ) between the two sinusoidal voltage sources for given values of myocardial properties ( $\sigma_1 = 2.22 \times 10^{-4} \text{S/mm}$ , and  $k_1 = 5.5 \times 10^{-4} \text{W}/(\text{mm} \cdot \text{K})$ , as listed in Table I) could be determined. Because the 3-D model in the previous case contained a large number of elements, it required very long computing time and large storage disk space for FEM analysis of bipolar phase-shifted MEC ablation. Thus, we opted to construct a 2-D model and utilize it to provide some preliminary understanding of bipolar phase-shifted MEC ablation.

The 2-D model was similar to the cross section of the 3-D model in Fig. 1. Fig. 2 shows the 2-D FEM model with three 12.5-mm electrodes (A and C on the opposite sides, and B in the middle). The width of the electrodes was 2.3 mm, and the interelectrode distance was also 2 mm. We define the optimal  $\phi$  as the phase difference between the two sinusoidal voltage sources—one delivered to A and C, the other to B—where the temperature at the outer edges ( $T_e$ ) and the temperatures adjacent to electrode B  $T_m$  are the same ( $T_e/T_m = 1$ ). For  $T_e$  and  $T_m$  we chose the maximum temperature of the hot spots at electrode edge and between the electrodes, respectively. We selected a duty cycle time period of 2 s for the sinusoidal voltage sources. We simulated the sinusoidal voltage source by dividing each duty cycle time period into seventeen 0.1176-s steps. During each of the 17 steps, the applied voltage was constant. The total ablation duration was 30 s (15 cycles in total) thus there were 255 steps in total. However, after submitting a time step to the FEM solver software, the software divides the step further into

small increments (i.e., one step does not correlate to the size of temporal discretization of the FEM model). Each 30-s constant voltage amplitude ablation would require approximately 250 min computing time. For the 3-D FEM model in the previous case, 255 steps would require in excess of 250 h of computing time. We applied one voltage source to electrode B, and applied the phase-shifted voltage source to the electrodes A and C. The model contained 22 055 nodes and 11 105 triangular elements. We performed postprocessing of the FEM results with ABAQUS/POST.

Since the purpose of this analysis was to determine the optimal  $\phi$  for our 2-D FEM model, we tested several phase-shifts and observed the temperature distributions and the ratios of  $T_e/T_m$ . Initially, we ran the simulations for  $\phi = 0^\circ, 10^\circ, 20^\circ, 30^\circ, 40^\circ,$  and  $45^\circ$ . Using trial-and-error, we also varied the amplitudes of the voltage generators between 60 and 90 V to until we obtained a maximum myocardial temperature of  $80^\circ\text{C}$  after 30 s for each  $\phi$ . Based on these initial results, we performed additional simulations until we found the optimal  $\phi$ .

#### D. Effect of Changes in Myocardial Properties

Based on the 2-D model in Section II-C, we performed similar FEM analyses but altered the myocardial electric and thermal conductivities. By trial and error, we performed repeated numerical analyses by changing the amplitude of the voltage generators so that the maximum myocardial temperature was  $80^\circ\text{C}$  after 30-s ablation. We varied myocardial electric conductivity in the following ways.

- 1) Increase the electric conductivity by 50% ( $1.5\sigma_1$ ).
- 2) Decrease the electric conductivity by 50% ( $0.5\sigma_1$ ).

Similarly, we also altered myocardial thermal conductivity.

- 3) Increase the thermal conductivity by 50% ( $1.5k_1$ ).
- 4) Decrease the thermal conductivity by 50% ( $0.5k_1$ ).

#### E. Change in Optimal Phase-Shift for MEC With Interelectrode Spacing

We also studied the effect of interelectrode distance by creating a similar 2-D FEM model similar to the model in Fig. 2 with an interelectrode spacing of 3 mm (versus 2 mm in the previous cases). We simulated  $\phi$  for  $10^\circ, 20^\circ, 30^\circ, 40^\circ,$  and  $45^\circ$  and performed additional simulations in order to determine the optimal  $\phi$ . The model had 24 755 elements and 11 905 nodes.

#### F. Temperature-Dependent Myocardial Properties and Temperature-Controlled Ablation

We included temperature-dependent myocardial properties in the 2-D model and simulated bipolar phase-shift MEC ablation in this case. We used a change of  $2\%/^\circ\text{C}$  of myocardial electric conductivity. We used the temperature-dependent thermal conductivity and the specific heat of the myocardium from Bhavaraju and Valvano [16], [17]. Similar to the previous case, we tried to adjust the amplitudes of the voltage generators to obtain a maximum myocardial temperature of  $80^\circ\text{C}$  after 30 s for each  $\phi$ .

In addition, we also performed a “true” temperature-controlled ablation for the bipolar phase-shifted MEC technique.

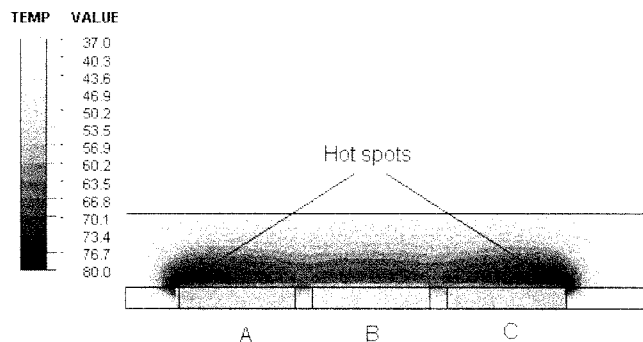


Fig. 3. Temperature distribution of the 3-D FEM model of unipolar MEC ablation. The temperatures at regions adjacent to the upper left corner of A and the upper right corner of B are highest ( $\sim 80^\circ\text{C}$ ).

This was again done by adjusting the applied voltage by trial-and-error, as described in Section II-B. For the first sinusoidal voltage cycle (0–2 s), we assigned the optimal  $\phi$  obtained from Section II-C, and performed repeated simulations in order to yield a maximum myocardial temperature of  $80^\circ\text{C}$  at the end of the cycle. For every duty cycle period (2 s) thereafter, we performed the following: 1) adjust the phase-shift between the two generators and 2) adjust the amplitude of the voltage generators to maintain the maximum myocardial temperature at  $80^\circ\text{C}$  throughout the 30-s ablation duration. We did not perform this temperature-controlled procedure for the other cases above, since a large amount of human interaction and trial-and-error simulations are necessary, simulation time would have exceeded acceptable limits.

### III. RESULTS

#### A. The Edge Effects Occur in Unipolar MEC

Fig. 3 shows the cross-sectional temperature profile of the 3-D FEM model described in Section II-B, after 30 s,  $80^\circ\text{C}$  temperature-controlled, unipolar RF ablation ( $\phi = 0$ ). The maximum temperature regions were adjacent to the upper left edge of electrode A, and, to the upper right of electrode C. The temperature distribution was symmetric between the center of the MEC. The maximum temperatures at areas of the hot spots adjacent to the edges of electrode B were lower ( $T_m \sim 54.1^\circ\text{C}$ ,  $T_e = 79.5^\circ\text{C}$ ). This result demonstrates that the edge effect also occurs in MEC (i.e., high temperatures are reached only at the outer edges of the outer electrodes). The amplitude of the voltage required to maintain  $80^\circ\text{C}$  maximum myocardial temperature throughout the whole simulation was in the range of 30 to 50 V. The computing time required to run this temperature-controlled analysis was approximately 100 h, due to required repeated simulations to maintain a set temperature.

#### B. Optimal Phase-Shift of a 2-D Bipolar MEC System

We performed FEM analyses for bipolar phase-shifted MEC ablation at  $\phi = 0^\circ, 10^\circ, 20^\circ, 30^\circ, 40^\circ,$  and  $45^\circ$  and calculated  $T_e/T_m$  for each case.  $T_e/T_m$  ranged from 1.53 at  $\phi = 0^\circ$  to 0.69 at  $\phi = 45^\circ$ . By trial-and-error, we simulated additional cases at  $\phi = 25^\circ, 26^\circ, 26.5^\circ,$  and  $27^\circ$ , and found that

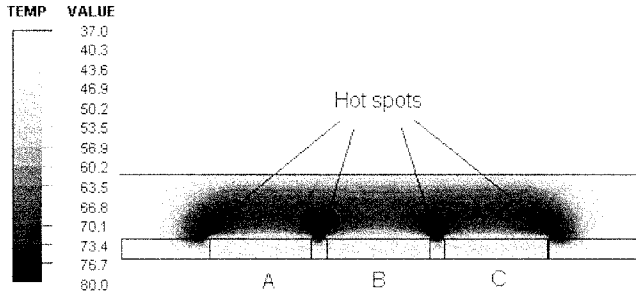


Fig. 4. The temperature distribution for 2-D FEM model of bipolar phase-shifted MEC ablation ( $\phi = 26.5^\circ$ ) after 30 s. The maximum myocardial temperature was  $80^\circ\text{C}$  and the electrode spacing was 2 mm.  $T_e/T_m$  was 1 in this case.

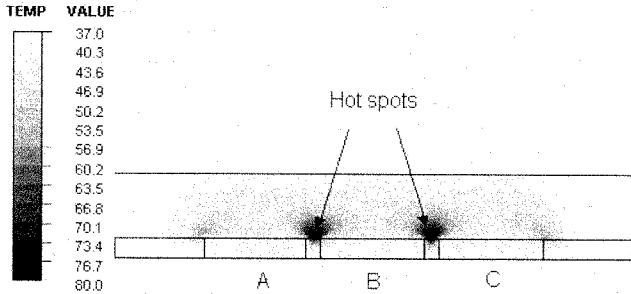


Fig. 5. The temperature distribution of the bipolar phase-shifted MEC ablation ( $\phi = 45.0^\circ$ ) after 30 s.  $T_e/T_m = 0.69$ .

the optimal  $\phi$  was  $26.5^\circ$  ( $T_e/T_m \approx 1$ ). The temperature distribution in the 2-D model at  $\phi = 0^\circ$  was similar to the result from the 3-D model cross-sectional temperature distribution (Fig. 3). Fig. 4 shows the myocardial temperature distribution of our 2-D bipolar phase-shifted MEC ablation FEM model, after 30 s,  $26.5^\circ$  phase-shifted bipolar ablation. We observe that the temperatures at all electrode edges are more uniform than those in the previous case, where only the outer electrode edges had high temperature (Fig. 3). Fig. 5 shows the temperature profile for the case where  $\phi = 45^\circ$ . In contrast to unipolar ablation (Fig. 3), the hot spots are located at the edges of electrode B.  $T_m$  in this case was  $\sim 80^\circ\text{C}$ , while  $T_e$  was  $55.2^\circ\text{C}$ .

### C. Optimal Phase Shift Versus Myocardial Properties

By repeating a similar computational method with the 2-D model outlined in Section II-C, We changed the myocardial properties and obtained their numerical results. Fig. 6 shows a plot of  $\phi$  versus  $T_e/T_m$  for different myocardial electrical conductivities; control ( $\sigma_1$ ), low ( $0.5\sigma_1$ ), and high ( $1.5\sigma_1$ ). The optimal  $\phi$  for the control case was  $26.5^\circ$ , while the optimal  $\phi$ 's for the low and high cases were  $29.5^\circ$ , and  $23.5^\circ$ , respectively. Fig. 7 shows the relationship between the optimal  $\phi$  and  $T_e/T_m$  for different myocardial thermal conductivities. The optimal  $\phi$ 's for all the cases were approximately  $26.5^\circ$ .

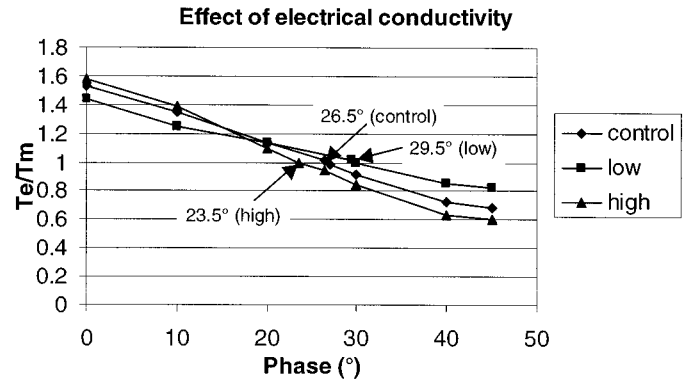


Fig. 6. Phase shifts versus temperature ratios. The optimal phases for control, low, and high electric conductivities are  $26.5^\circ$ ,  $29.5^\circ$ , and  $23.5^\circ$ , respectively.

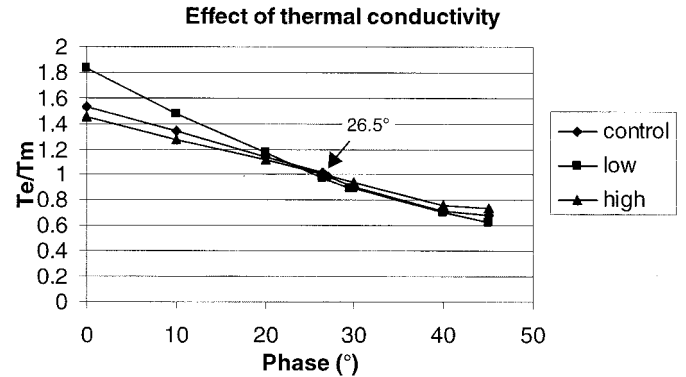


Fig. 7. The optimal phases for different cases of myocardial thermal conductivities. The optimal phases for all cases are similar ( $\sim 26.5^\circ$ ).

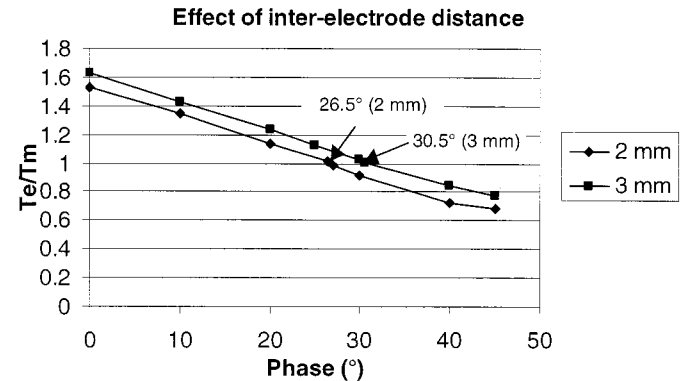


Fig. 8. The effect of interelectrode distances. The optimal phase for 2-mm spacing is  $26.5^\circ$ , while the optimal phase for 3-mm spacing is  $30.5^\circ$ .

### D. Optimal Phase-Shift Versus Interelectrode Spacing

Fig. 8 shows the relationship between  $\phi$  and  $T_e/T_m$  for 3-mm and 2-mm spacings. The ratios  $T_e/T_m$  in 3-mm spacing MEC were consistently higher than those of 2-mm MEC spacing. The optimal  $\phi$  for 3-mm spacing was  $30.5^\circ$  ( $26.5^\circ$  when the inter-electrode distance was 2 mm).

### E. Effects of Temperature-Dependent Myocardial Properties and Temperature-Controlled Ablation

When we included temperature-dependent properties into our 2-D FEM model, we could obtain  $T_e/T_m = 1$  after 30-s ablation by setting  $\phi = 23.5^\circ$ . However, unlike the results of temperature

independent myocardial properties in Section III-B–D,  $T_e/T_m$  varied from 1.27 after 2 s, to 1.0 after 30-s (at  $\phi = 23.5^\circ$ ). The ratios of  $T_e/T_m$  were essentially the same throughout ablation duration in the previous cases A through D. The amplitude of both voltage generators used was 59.8 V in order for the maximum myocardial temperature to be 80 °C after 30 s.

For temperature-controlled ablation, we used  $\phi = 26.5^\circ$  as obtained in Section III-B for the first duty cycle time period.  $T_e/T_m$  after 2-s ablation was 0.83. We set the amplitude of the voltage generators to 97 V in order for the maximum myocardial temperature to be 80 °C after 2 s. By trial-and-error, we adjusted  $\phi$  to 24.0° for the next duty cycle time period (2–4 s) in order to have  $T_e/T_m = 1$ . For the rest of the ablation duration, we varied the amplitude of the voltage generators in the range of 70 to 90 V. The phase-shift was adjusted in a small range (23° to 24°) in order to maintain  $T_e/T_m$  at 1.0 after every duty cycle time period.

#### IV. DISCUSSION

The result from our 3-D FEM model demonstrates the undesirable edge effect in unipolar MEC RF ablation. This could lead to overheating or noncontinuous linear lesions when the unipolar MEC ablation approach is applied to cure AFIB in clinical practice. We could create deeper and more uniform lesions by maintaining the same temperature at all electrode edges, as already proven by *in vivo* studies [18], [19]. For bipolar phase-shifted MEC ablation, we used two voltage generators and delivered them to different electrodes on the MEC. By determining the optimal phase-shift between the two generators, we could maintain the same temperatures at all of the electrode edges. This also leads to deeper lesions above the middle section of the catheter. When the voltage applied to electrodes A and C has some phase shift compared with the voltage applied to electrode B, there will be differences in the current distribution. Since now electrodes A and C are at a different potential than electrode B, there will be current flow between the electrodes in addition to current flow from each of the electrodes toward ground. The current flow between the electrodes will be maximal at 180° phase-shift, and zero at 0° phase-shift. This interelectrode current will preferentially heat up the tissue in-between the electrodes and allow additional power deposition at these locations, dependent on the phase shift. Therefore, we take the variable  $T_e/T_m$  to determine optimal phase-shift. When  $T_e/T_m = 1$ , both hot spots have the same maximal temperature, and we get maximum dissipated power. Ideally, we would try to keep  $T_e/T_m = 1$  during the whole ablation procedure. For the results presented in Section II-B–D, however we only optimized  $T_e/T_m = 1$  at the end of the ablation procedure, to get initial approximations of optimal  $T_e/T_m$ . As the results in Section II-E show, where we kept  $T_e/T_m = 1$  all the time, the phase-shift has to be varied only within a small range, so the results presented in Section II-B–D provide good approximations.

The optimal phase-shift decreased as we increased the myocardial electric conductivity and increased as we decreased the electric conductivity. When we included temperature-dependent

myocardial properties and performed bipolar phase-shifted ablation at a fixed  $\phi$ ,  $T_e/T_m$  changed over time due to the rise in tissue temperature. Thus, constant amplitude voltage sources are incapable of maintaining  $T_e/T_m$  to 1.0 when the myocardial properties are temperature dependent. Our numerical results also showed that different interelectrode spacings had different optimal phase-shift.

In this study, we chose 2 s as the duty cycle time period for the sinusoidal voltage sources. In order to limit the computing time required for each analysis. In clinical settings, a much shorter cycle can be applied (considering for 500 kHz, the time period would be 2  $\mu$ s). For our simulation to be accurate, the time period has to be lower than the time constant associated with the temperature rise. Otherwise the changes in current flow will be too slow and result in incorrect temperature distribution. In order to limit the computing time required for each analysis, we chose a 2-s time period as a compromise, even though it is within the range of the time constant.

The simplest way to implement bipolar phase-shifted MEC is to apply two constant amplitude sinusoidal voltage generators at a fixed phase-shift (e.g., at 25°) for the entire ablation duration. Another possible implementation of bipolar phase-shifted ablation is the following. We set the phase-shift between the two voltage generators to 25° initially, and utilize an algorithm to adjust the phase-shifts for the next cycles. If  $T_e > T_m$ , we increase the phase-shift and if  $T_e < T_m$ , we reduce the phase-shift. This will help increase the uniformity of the temperature distribution along the MEC. We can also operate bipolar phase-shifted ablation under temperature-controlled RF ablation by simultaneously adjusting the phase and the amplitude of the sinusoidal voltage generators to maintain uniform temperature at a desired preset value. Note that, although the magnitudes of the two generators at a given instant might have been different, the peak amplitudes of the sinusoidal voltage sources in every simulation we performed were always the same.

Note that the results using the 2-D FEM models presented in this paper are only qualitative in nature. The transition from 3-D to 2-D introduces some error. Another error is introduced by choosing a time period of the applied voltage of 2 s. This time lies within the range of the time constant of thermal heating. Furthermore, we used no real temperature control in the experiments in Section II-B–D which might introduce some error. Nevertheless, the simulation demonstrates the general effects of change in phase angle of applied voltage and how tissue properties and interelectrode distance affect optimal phase angle.

We demonstrated by simulation using a 3-D FEM model that temperature at the outer electrode edges exceeds the temperature at the inner electrode edges. We show, that these temperatures can be equalized using phase-shifted application of voltage with 2-D FEM models resulting in higher temperatures in between the electrodes compared with unipolar application. Studies performed by other researchers already showed experimentally that phase-shifted mode can create deeper and more uniform lesions than unipolar mode. We provide results showing the qualitative relationship between optimal phase-shift and other parameters such as myocardial properties and interelectrode spacing. These results give some insight on how to design control for MEC utilizing

phase-shifted voltage application and may provide useful to direct future experimental designs studying phase-shifted MEC.

## REFERENCES

- [1] S. L. Kopecky, B. J. Gersh, M. D. McGoon, J. P. Whisnant, D. R. Holmes Jr, D. M. Ilstrup, and R. L. Frye, "The natural history of lone atrial fibrillation: A population-based study over 3 decades," *N. Eng. J. Med.*, vol. 17, pp. 669–674, 1987.
- [2] C. D. Furberg, B. M. Psaty, T. A. Manolio, J. M. Gardin, V. E. Smith, and P. M. Rautaharju, "Prevalence of atrial fibrillation in elderly subjects (the Cardiovascular Heath Study)," *Amer. J. Cardiol.*, vol. 74, pp. 236–241, 1994.
- [3] S. K. S. Huang and D. J. Wilber, Eds., *Radiofrequency Catheter Ablation of Cardiac Arrhythmias: Basic Concepts and Clinical Applications*, 2nd ed. Armonk, NY: Futura, 2000.
- [4] J. L. Cox, R. B. Schuessler, M. E. Cain, P. B. Corr, C. M. Stone, H. J. D'Agostino Jr, A. Harada, B. C. Chang, P. K. Smith, and J. P. Boineau, "Surgery for atrial fibrillation," *Sem. Thorac. Cardiovasc. Surg.*, vol. 1, pp. 67–73, 1989.
- [5] J. L. Cox, "The surgical treatment of atrial fibrillation IV: surgical technique," *J. Thorac. Cardiovasc. Surg.*, vol. 101, pp. 584–592, 1991.
- [6] M. Haissaguerre, P. Jais, D. C. Shah, A. Takahashi, M. Hocini, G. Quiniou, S. Garrigue, A. Le Mouroux, P. Le Metayer, and J. Clementy, "Spontaneous initiation of atrial fibrillation by ectopic beats originating in the pulmonary veins," *N. Eng. J. Med.*, vol. 339, pp. 659–666, 1998.
- [7] F. X. Roithinger, P. R. Steiner, Y. Goseki, K. S. Liese, D. B. Scholtz, A. Sippensgroenewegen, P. Ursell, and M. D. Lesh, "Low power radiofrequency application and intracardiac echocardiography for creation of continuous left atrial linear lesions," *J. Cardiovasc. Electrophysiol.*, vol. 10, pp. 680–680, 1999.
- [8] I. D. McRudy, D. Panescu, M. A. Mitchell, and D. E. Haines, "Nonuniform heating during radiofrequency catheter ablation with long electrodes: monitoring the edge effect," *Circulation*, vol. 96, pp. 4057–4064, 1997.
- [9] L. M. Epstein, M. A. Mitchell, T. W. Smith, and D. E. Haines, "Comparative study of fluoroscopy and intracardiac echocardiographic guidance for the creation of linear atrial lesions," *Circulation*, vol. 98, pp. 1796–801, 1998.
- [10] S. N. Goldberg, M. C. Stein, G. S. Gazelle, R. G. Sheiman, J. B. Kruskal, and M. E. Clouse, "Percutaneous radiofrequency tissue ablation: Optimization of pulsed radiofrequency technique to increase coagulation necrosis," *J. Vasc. Interv. Radiol.*, vol. 10, pp. 907–916, 1999.
- [11] W. Sun, "Finite element analysis of temperature profiles in linear phased multi-electrode ablation," in *Proc. 20th Annu. Int. Conf. IEEE Eng. Med. Biol. Soc.*, Hong Kong, 1998, pp. 252–255.
- [12] D. Panescu, S. D. Fleischman, J. G. Wayne, D. K. Swanson, M. S. Mirotznik, I. McRury, and D. E. Haines, "Radiofrequency multielectrode catheter ablation in the atrium," *Phys. Med. Biol.*, vol. 44, pp. 899–915, 1999.
- [13] S. Nath, C. Lynch III, J. G. Wayne, and D. E. Haines, "Cellular electrophysiological effects of hyperthermia on isolated Guinea pig papillary muscle: Implications for catheter ablation," *Circulation*, pt. 1, vol. 88, pp. 1826–1831, 1993.
- [14] M. K. Jain and P. D. Wolf, "A three-dimensional finite element model of radiofrequency ablation with blood flow and its experimental validation," *Ann. Biomed. Eng.*, vol. 28, pp. 1075–84, 2000.
- [15] E. J. Woo, S. Tungjitkusolmun, H. Cao, J.-Z. Tsai, J. G. Webster, V. R. Vorperian, and J. A. Will, "A new catheter design using needle electrode for subendocardial RF ablation of ventricular muscles: finite-element analysis and *in vitro* experiments," *IEEE Trans. Biomed. Eng.*, vol. 47, pp. 23–31, Jan. 2000.
- [16] K. R. Foster and H. P. Schwan, "Dielectric properties of tissues and biological materials: a critical review," *CRC Crit. Rev. Biomed. Eng.*, vol. 17, pp. 25–104, 1989.
- [17] N. C. Bhavaraju and J. W. Valvano, "Thermophysical properties of swine myocardium," *Int. J. Thermophys.*, vol. 20, pp. 665–76, 1999.
- [18] X. Zheng, R. E. Ideker, J. A. Hall, D. L. Rollins, and G. P. Walcott, "Creation of uniform linear lesions by phased radiofrequency energy," in *Proc. BMES 2000 Conf.*, Seattle, WA, 2000.
- [19] X. Zheng, G. P. Walcott, D. L. Rollins, J. A. Hall, W. M. Smith, G. N. Kay, and R. E. Ideker, "Different tissue heating effectiveness of phased and nonphased radiofrequency energy during linear ablation," *J. Amer. Coll. Cardiol.*, vol. 35, pp. 111A–112A, 2000.
- [20] J. A. Hall, G. P. Walcott, H. Kurtz, M. Sherman, W. Bowe, J. Simpson, T. Castellano, and G. N. Kay, "Pathology of atrial ablation lesions created utilizing temperature monitored phased radio frequency energy: periacute and chronic results," *PACE*, vol. 21, p. 963, 1998.
- [21] G. P. Walcott, J. A. Hall, G. N. Kay, K. Ellenbogen, M. Wood, and H. Calkins, "Linear phased radiofrequency catheter ablation in the left and right atria for the treatment of atrial fibrillation," in *Proc. BMES 2000 Conf.*, Seattle, WA, 2000.
- [22] J. L. Cox, R. B. Schuessler, H. J. D'Agostino, C. M. Stone, B. C. Chang, M. E. Cain, P. B. Corr, and J. P. Boineau, "The surgical treatment of atrial fibrillation: development of a definitive surgical procedure," *J. Thorac. Cardiovas. Surg.*, vol. 101, pp. 569–583, 1991.
- [23] D. E. Haines and S. Nath, "New horizons in catheter ablation," *J. Interv. Cardiol.*, vol. 8, pp. 845–856, 1995.
- [24] H. H. Pennes, "Analysis of tissue and arterial blood temperatures in resting forearm," *J. Appl. Phys.*, vol. 1, pp. 93–122, 1948.



**Supan Tungjitkusolmun** (S'96–M'00) was born in Bangkok, Thailand, December 5, 1972. He received the B.S.E.E. degree from the University of Pennsylvania, Philadelphia, in 1995, and the M.S.E.E. and Ph.D. degrees from the University of Wisconsin, Madison, in 1996, and 2000.

He is on the faculty of the Department of Electronics, Faculty of Engineering, and the Research Center for Communications and Information Technology, King Mongkut's Institute of Technology Ladkrabang, Bangkok, Thailand. His research

interests include finite-element modeling, radio-frequency cardiac ablation, and hepatic ablation.

He is a member of Tau Beta Pi, Eta Kappa Nu, and Pi Mu Epsilon.



**Dieter Haemmerich** (S'00) was born in Vienna, Austria on May 22, 1971. He received the B.S.E.E. degree from the Technical University of Vienna, Austria in 1997 and the M.S.B.M.E. degree from the University of Wisconsin, Madison, in 2000. He is currently working toward the Ph.D. degree in the Department of Biomedical Engineering, University of Wisconsin.

His research interests include finite-element analysis of radio frequency ablation and tissue impedance measurement.



**Hong Cao** (S'97) received the B.S. and M.S. degrees in electrical engineering from Nanjing University, Nanjing, China in 1992 and 1995, respectively. He received the Ph.D. degree in electrical and computer engineering at the University of Wisconsin, Madison, in 2001.

Currently, he is a Senior Software Developer at Epic System Corporation, working on enterprise electronic medical record (EMR) database system and integration of medical instruments into EMR system. His research interests include medical instrumentation, RF catheter ablation of cardiac tissue and hepatic tumor, and medical information system.

He is contributing author to J. G. Webster (Ed.), *Minimally Invasive Medical Technology* (Bristol, U.K.: IOP Publishing, 2001).



**Jang-Zern Tsai** (S'97) was born in Chia-Yi, Taiwan, in 1961. He received the B.S.E.E. degree from National Central University, Chung-Li, Taiwan, in 1984, and the M.S.E.E. degree from National Tsing Hua University, Hsinchu, Taiwan, in 1986. In 2001, he received the Ph.D. degree in electrical and computer engineering from the University of Wisconsin, Madison, doing research on myocardial resistivity measurement.

He joined the Industrial Technology Research Institute (ITRI) as an Integrated Circuit Applications Engineer and as a Hardware Engineer on digital recording technology. In 1990, he joined the Computer and Communication Research Laboratories of ITRI as a Hardware Engineer on digital recording technology and the Accton Technology Corporation as a Software Engineer. He is presently a Postdoctoral Fellow at the University of California developing hardware for electrical impedance tomography



**Young Bin Choy** (SM'00) was born in Seoul, Korea on Aug 17, 1976. He received the B.S. degree from the School of Electrical Engineering, Seoul National University, Seoul, Korea, in 1999. He received the M.S.E.E degree in 2000 from the University of Wisconsin-Madison on research measuring the mechanical compliance of the endocardium to determine the relation between the penetration depth of the RF cardiac catheter ablation electrode and the force. He is currently working toward the Ph.D. degree at the University of Illinois at Urbana-Champaign.

He was an Engineer with LG Corporate Institute of Technology from January to June 1999.



**Vicken R. Vorperian** received the M.D. degree in 1985 from the American University of Beirut, Lebanon. He did a fellowship in cardiac arrhythmias and electrophysiology at the Vanderbilt University, Nashville, TN; and fellowship in cardiac pacing and catheter ablation at the University of Michigan, Ann Arbor, MI.

He is Clinical Associate Professor of Medicine in the Department of Medicine, University of Wisconsin-Madison and is an electrophysiologist in the Cardiac Electrophysiology Laboratory at the University of Wisconsin Hospital. He is also a member of the Arrhythmia Consultants of Milwaukee S.C., a private practice group in cardiac arrhythmias and clinical cardiac electrophysiology.



**John G. Webster** (M'59-SM'69-F'86-LF'97) received the B.E.E. degree from Cornell University, Ithaca, NY, in 1953, and the M.S.E.E. and Ph.D. degrees from the University of Rochester, Rochester, NY, in 1965 and 1967, respectively.

He is Professor of Biomedical Engineering at the University of Wisconsin-Madison. In the field of medical instrumentation, he teaches undergraduate and graduate courses, and does research on radio-frequency cardiac and hepatic ablation.

Dr. Webster is editor of *Medical instrumentation: application and design*, 3rd edition (New York: Wiley, 1998), *Encyclopedia of electrical and electronics engineering* (New York: Wiley, 1999), and *Minimally invasive medical technology* (Bristol, U.K.: IOP Publishing, 2001). He is the recipient of the 2001 EMBS Career Achievement Award.